

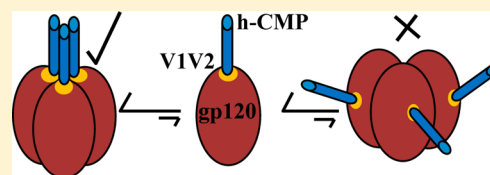
Designed Cyclic Permutants of HIV-1 gp120: Implications for Envelope Trimer Structure and Immunogen Design

Piyali Saha, Sanchari Bhattacharyya, Sannula Kesavardhana, Edward Roshan Miranda, P. Shaik Syed Ali, Deepak Sharma, and Raghavan Varadarajan*

Molecular Biophysics Unit, Indian Institute of Science, Bangalore 560 012, India

ABSTRACT: Most HIV-1 broadly neutralizing antibodies are directed against the gp120 subunit of the env surface protein. Native env consists of a trimer of gp120–gp41 heterodimers, and in contrast to monomeric gp120, preferentially binds CD4 binding site (CD4bs)-directed neutralizing antibodies over non-neutralizing ones. Some cryo-electron tomography studies have suggested that the V1V2 loop regions of gp120 are located close to the trimer interface. We have therefore designed cyclically permuted variants of gp120

with and without the h-CMP and SUMO2a trimerization domains inserted into the V1V2 loop. h-CMP-V1cyc is one such variant in which residues 153 and 142 are the N- and C-terminal residues, respectively, of cyclically permuted gp120 and h-CMP is fused to the N-terminus. This molecule forms a trimer under native conditions and binds CD4 and the neutralizing CD4bs antibodies b12 with significantly higher affinity than wild-type gp120. It binds non-neutralizing CD4bs antibody F105 with lower affinity than gp120. A similar derivative, h-CMP-V1cyc1, bound the V1V2 loop-directed broadly neutralizing antibodies PG9 and PG16 with ~20-fold higher affinity than wild-type JRCSF gp120. These cyclic permutants of gp120 are properly folded and are potential immunogens. The data also support env models in which the V1V2 loops are proximal to the trimer interface.



HIV-1 (human immunodeficiency virus) is the etiological agent of AIDS. Despite decades of extensive efforts, discovery of an immunogen capable of eliciting broadly neutralizing antibodies remains elusive. The neutralizing antibody response is primarily directed against the envelope (env) protein of HIV-1.^{1,2} HIV-1 is an RNA virus from the retroviridae family, and its trimeric env surface protein consists of two noncovalently associated subunits, membrane-anchored subunit gp41 and surface subunit gp120. The ectodomain of gp41 consists of two heptad repeats (N and C heptad repeats), a disulfide loop region, and a hydrophobic membrane proximal external region. Surface subunit gp120 consists of the inner domain, the outer domain, and bridging sheet regions.³ On the native env spike, the inner domain of gp120 interacts with the ectodomain of gp41. Upon interaction with cellular receptor CD4, gp120 undergoes conformational changes that lead to the exposure of cryptic epitopes (CD4i). Binding of gp120 to the coreceptors (CCR5 and CXCR4) on the target cell membrane leads to further conformational changes and ultimately to the fusion of viral and cellular membranes, driven by formation of a six-helix bundle on gp41.

Although gp120 is the target of several neutralizing antibodies, immunization with recombinant monomeric gp120 typically elicits antibodies that are able to neutralize T-cell line-adapted and other neutralization-sensitive viruses but not more resistant circulating primary isolates.⁴ This suggests that recombinant monomeric gp120 does not faithfully mimic the native env spike on the virion surface. A number of different approaches have been pursued to elicit broadly neutralizing antibodies against HIV-1 but so far have met with limited success.

The conserved coreceptor binding site on the env glycoprotein is involved in the attachment of the virus to the target cell membrane. However, epitopes in this region show increased levels of exposure after receptor binding. One approach to exposing these cryptic epitopes (CD4i epitopes) is to stabilize gp120 through CD4 binding.

Previous studies have shown that immunization with gp120–CD4 complexes or single chains was able to elicit neutralizing antibodies against HIV-1.^{5–9} We have previously shown that the broad neutralization elicited by the gp120–CD4 single chain was due to anti-CD4 antibodies.¹⁰ In the same study, a single chain of the gp120–M9 complex was also tested. M9 is a 27-residue scyllatoxin-derived mimic of the gp120 binding region of CD4. However the gp120–M9 single chain did not display CD4i epitopes or elicit neutralizing antibodies. It is possible that the use of a long flexible linker to connect the termini of gp120 and M9 might have affected the folding of the molecule. Hence, in this work, we report the reduction of linker length by cyclic permutation of gp120 and characterization of the single-chain derivatives of these cyclic permutants with M9.

To elicit broadly neutralizing antibodies against HIV-1 env, several strategies have been employed to mimic the native, trimeric, gp120–gp41 spike on the virion surface. These include the design of cleavage defective gp140, cleavage competent gp140 stabilized by disulfide linkage between gp120 and gp41 (SOSgp140 and SOSIPgp140),^{11–13} fusion of trimerization domains with gp140¹⁴ and gp120,¹⁵ formation

Received: January 2, 2012

Revised: February 9, 2012

Published: February 13, 2012



of HIV and SIV chimeric gp140,¹⁶ stabilization of gp140 by introduction of cysteine mutations into the gp41 N heptad repeat region,¹⁷ and addition of a trimerization domain at the C-terminus of gp140 or gp130 along with cysteine mutations in gp41^{18,19} to facilitate trimer formation. Several of the designed mutants were largely trimeric. However, the sera elicited by the uncleaved gp140–GCN4 complex at best showed only marginal improvements in neutralization affinity relative to those elicited by monomeric gp120.²⁰ Subsequently, it was shown²¹ that cleavage of cell surface-displayed gp160 is essential for formation of a nativelylike trimer, which binds CD4bs-directed neutralizing antibodies such as b12 considerably better than corresponding non-neutralizing ones. Recently, Liu et al. modeled the HIV-1 env spike on the virion surface using cryo-electron tomography.²² By fitting various ligand-bound crystal structures of gp120 into the tomogram, they demonstrated how each gp120 monomer is oriented in the native env spike. In the native, unliganded spike, truncated V1V2 loops from each gp120 subunit are oriented toward the excess electron density at the apex of the trimer. The trimer appears to be held together by strong contacts at the base involving gp41, and at the apex that appears to be largely mediated by the V1V2 loop. However, other cryo-EM microscopy and tomogram studies have made conflicting claims.^{22–26} In our work, we also report the design and stabilization of circularly permuted gp120 in a trimeric conformation. Trimerization was achieved by fusion of gp120 with two different trimerization domains (h-CMP and SUMO2a) inserted into the V1 loop. The binding of the trimeric constructs to various neutralizing and non-neutralizing antibodies was characterized. These trimeric constructs are novel, potential immunogens against HIV-1. The data also support models of the HIV-1 spike in which the V1V2 loops are proximal to the trimer interface.

■ EXPERIMENTAL PROCEDURES

Construct Descriptions. The gp120 sequences (amino acids 31–511) used in this work are derived from the JRFL and JRCSF isolates. Gene sequences were codon optimized for expression in mammalian cells. M9 is a 27-residue CD4 analogue based on a scyllatoxin scaffold. It is a structural mimic of β -strands C' and C'' of domain D1 of human CD4. M9 binds gp120 ~100-fold less strongly than CD4.²⁷ h-CMP is a 43-residue peptide consisting of the coiled coil domain of human cartilage matrix protein,²⁸ which assembles into a homotrimer. SUMO2a is a mutant of the 72-residue human SUMO2 protein²⁹ and contains two designed cysteine mutations at positions 26 and 46 to stabilize the homotrimeric form of the protein via disulfide bond formation.

Cloning of Cyclic Permutants. To cyclically permute gp120, new N- and C-termini were chosen at the V1V2, V3, and V4 loop regions, and the original N- and C-termini of wt-gp120 were connected via a 20-amino acid linker. V1Jnstpagp120-L-CD4D12¹⁰ was used as a template. Here L is a 20-residue linker composed of repeats of the GSA tripeptide sequence. In this template, gp120 was cloned between BglII and XbaI restriction sites and CD4D12 between BamHI and KpnI restriction sites. For the cyclic permutants, the N-terminal fragments (residues 153–511 for V1cyc, 328–511 for V3cyc, and 409–511 for V4cyc) were amplified with BglII and XbaI restriction sites at the N- and C-termini, respectively. The C-terminal fragments (residues 31–142 for V1cyc, 31–305 for V3cyc, and 31–401 for V4cyc) were

amplified with BamHI and KpnI restriction sites at the N- and C-termini, respectively. The polymerase chain reaction (PCR) products for each cyclic permutant and template V1Jnstpagp120-L-CD4D12 were digested with BglII and XbaI restriction enzymes and ligated to generate the N-terminal fragment of the cyclic permutants. Similarly, the PCR products and the template V1Jnstpagp120-L-CD4D12 were digested with BamHI and KpnI restriction enzymes and ligated to generate the C-terminal fragment of the cyclic permutants. Individual N and C fragments of the cyclic permutants were ligated together to generate three different cyclic permutants.

Cloning of Single-Chain Derivatives of the Cyclic Permutants. To generate single-chain derivatives of the cyclic permutants and M9, V1Jnstpagp120-L-M9,¹⁰ V1JnstpaV1cyc, and V1JnstpaV3cyc were used as templates. In the case of V1cyc and V3cyc, the stop codon at the end of the gene was mutated using megaprimer-based PCR³⁰ to introduce an NheI restriction site. To have appropriate linkers between cyclic permutants and M9, an NheI restriction site was introduced at the required positions in the linker region of V1Jnstpagp120-L-M9 by a similar megaprimer-based PCR. All templates containing the NheI restriction site were doubly digested with HpaI and NheI restriction enzymes, and inserts from V1cyc and V3cyc were ligated into the doubly digested vectors of gp120-L-M9 having 7- and 12-amino acid linkers, respectively.

Cloning and Gene Synthesis of Oligomeric Cyclic Permutants. Two different trimerization domains, h-CMP and SUMO2a, were fused individually at the N-terminus of V1cyc. Both trimerization domains were constructed by gene synthesis and amplified via PCR with BglII restriction sites at the N- and C-termini. The V1JnstpaV1cyc vector and PCR products containing the trimerization domains were digested with BglII and ligated to generate h-CMP-V1cyc and SUMO2a-V1cyc. Only three amino acids (EIS) encoded by the restriction sites lie between the trimerization sequence and the N-terminus of the JRFL cyclic permutant. The E168K mutation was also introduced into both constructs. Genes for wt-gp120, h-CMP-V1cyc1, and V2cyc-h-CMP, based on the JRCSF sequence of HIV-1, were synthesized by Genscript and were human codon-optimized. In this case, two amino acids (AS) lie between the trimerization sequence and the cyclic permutants.

Cell Lines, Antibodies, and Reagents. The HEK293 cell line was obtained from the National Centre for Cell Sciences (Pune, India). Monoclonal antibody (mAb) IgG-b12 was obtained from Neutralizing Antibody Consortium of the International AIDS vaccine Initiative (IAVI, New York, NY). Antibodies PG9 and PG16 were kindly provided by S. Phogat. Antibody F105 was kindly provided by L. Cavacini. Polyclonal antisera against gp120 were generated in rabbits as described previously.³¹

Expression and Purification of gp120 Derivatives. Plasmids of all the constructs were transiently transfected into HEK293 cells by using the polyfect transfection reagent (Qiagen) according to the manufacturer's protocol. Eight hours after transfection, the medium was replaced with OptiMem reduced serum medium (Gibco). After an additional 48–72 h, supernatants were collected and analyzed for protein expression by anti-gp120 immunoblot assays. Proteins were purified by affinity chromatography using Lentil-Lectin Sepharose 4B (Amersham-Pharmacia Biotech). Bound protein was eluted with 600 mM α -D-methyl mannopyranoside in PBS (pH 7.4). Protein concentrations were determined by a BCA

assay (Sigma) according to the manufacturer's protocol using BSA as a standard.

BN-PAGE, SDS–PAGE, and Western Blot Analysis. JRFLgp120, V1cyc, h-CMP-V1cyc, SUMO2a-V1cyc, h-CMP-V1cyc1, V2cyc-h-CMP, and JRCSF gp120 were analyzed under nonreducing conditions using BN-PAGE; 5× sample buffer [250 mM MOPS, 250 mM Tris-HCl (pH 7.7), 40% glycerol, and 0.1% Coomassie brilliant blue G250] was added to the samples prior to them being loaded onto a 4 to 12% Bis-Tris NuPAGE gel (Invitrogen). Samples were electrophoresed at 4 °C for 3 h at 100 V. The cathode buffer contained 50 mM MOPS, 50 mM Tris (pH 7.7), and 0.002% Coomassie brilliant blue G250, and the same buffer without Coomassie brilliant blue G250 served as the anode buffer. The gel was then blotted onto a polyvinylidene difluoride (PVDF) membrane (Millipore), which was then washed with a 30% methanol/10% acetic acid mixture followed by 100% methanol to remove excess Coomassie blue dye from the membrane. A broad range molecular weight protein ladder (Invitrogen) was used as the molecular weight marker.

Electrophoretic analysis of denatured envelope glycoproteins was performed using 6% SDS–PAGE. Samples were denatured by being boiled for 10 min in sample buffer (2% SDS, 40% glycerol, and 0.1% Coomassie brilliant blue R250) and subjected to 6% SDS–PAGE with and without DTT. Proteins were then electrophoretically transferred to a PVDF membrane. A broad range protein ladder (Invitrogen) was used as a molecular weight marker. Following blotting, membranes were blocked with 5% nonfat milk (Bio-Rad) in phosphate-buffered saline (PBS, pH 7.4) for 2 h at room temperature. The membranes were washed thrice with PBS containing 5% nonfat milk and 0.05% Tween 20 and then incubated with anti-gp120 antisera generated in rabbits (1:1000) in a 5% milk/PBS mixture at 4 °C for 5 h. The membranes were again washed three times with PBS containing 5% nonfat milk and 0.05% Tween (PBST) and incubated with horseradish peroxidase-conjugated anti-rabbit antibody (Sigma-Aldrich, 1:10000 dilution) in a 5% milk/PBS mixture for 2 h at 4 °C, and the membranes were then washed with PBST solution. Bound antibody was detected with amino ethyl carbazole (Sigma-Aldrich) and hydrogen peroxide.

Biacore Experiments. All Biacore experiments were performed with a Biacore 2000 (Biacore, Uppsala, Sweden) optical biosensor at 25 °C. In the first assay, 1000 resonance units (RU) of four-domain CD4 was attached by amine coupling to the surface of a research-grade CM5 chip (GE Healthcare). The binding of gp120 and its derivatives to this surface was examined. A naked sensor surface without antibody that was activated and deactivated served as a negative control for each binding interaction. gp120 and its derivatives, which had been serially diluted, were run across each sensor surface at four different concentrations in a running buffer of PBS with 0.005% P20. Protein concentrations ranged from 12.5 to 75 nM for gp120, from 4 to 25.2 nM for V1cyc, from 5.6 to 29.4 nM for V3cyc, and from 5.4 to 34 nM for V4cyc. For the remaining proteins, interactions were studied at concentrations ranging from 60 to 180 nM for single-chain derivatives (V1cyc-M9 and V3cyc-M9) and at concentrations of 2–8 nM for two other trimerized cyclic permutants of gp120 (h-CMP-V1cyc and SUMO2a-V1cyc).

In the second assay, 1000 RU of IgG-b12 was attached by amine coupling to the surface of a research-grade CM5 chip and interaction with JRFL wt gp120, monomeric and

oligomeric V1cyc was examined. Three serial dilutions of V1cyc and SUMO2a-V1cyc and four serial dilutions of wt gp120 and h-CMP-V1cyc were run across the sensor surface in running buffer of PBS and 0.005% P20. Protein concentrations ranged from 50 to 200 nM for wt gp120, from 30 to 90 nM for V1cyc, from 80 to 240 nM for h-CMP-V1cyc, and from 200 to 600 nM for SUMO2a-V1cyc. In the third assay, 1000 RU of IgG-F105 was immobilized on the research-grade CM5 chip and interactions with wt gp120, V1cyc and its derivatives were examined. Proteins were serially diluted, and binding was studied for three different concentrations of V1cyc and its derivatives. Protein concentrations ranged from 50 to 300 nM for wt gp120, 15 to 45 nM for V1cyc, from 40 to 120 nM for h-CMP-V1cyc, and from 100 to 300 nM for SUMO2a-V1cyc. Binding and dissociation were measured for 100 s each, at a flow rate of 30 μ L/min. For four-domain CD4 and F105, the sensor surface was regenerated between binding reactions by one to two washes with 10 mM NaOH for 60 s at a rate of 10 μ L/min, and for IgG-b12, the sensor surface was regenerated between binding reactions by washes with 10 mM HCl for 60 s at a rate of 10 μ L/min. Each binding curve was corrected for nonspecific binding by subtraction of the signal obtained from the negative-control flow cell.

In the fourth assay, 1500 RU of IgG-PG9 or IgG-PG16 was immobilized on the research-grade CM5 chip and interactions with JRCSFgp120 and h-CMP-V1cyc1 were examined. Proteins were serially diluted, and interactions were studied for three different concentrations of JRCSF gp120. For PG9 and PG16, the concentration of JRCSF gp120 was varied from 410 nM to 1.6 μ M and that of h-CMP-V1cyc1 from 208 nM to 2.55 μ M. In all cases, the flow rate was 20 μ L/min. For PG9 and PG16, the sensor surface was regenerated between binding reactions by one or two washes with 4 M MgCl₂ for 10 s at a rate of 30 μ L/min. The kinetic parameters were obtained by fitting the data to the simple 1:1 Langmuir interaction model by using BIA EVALUATION version 3.1. All the Biacore experiments were conducted at least twice.

RESULTS

Design of Cyclic Permutants of JRFL gp120. We have previously reported the design of single-chain derivatives of gp120 with CD4D12 or M9 in an attempt to construct immunogens with exposed CD4i epitopes.¹⁰ Although sera from guinea pigs immunized with gp120-CD4D12 were able to neutralize various HIV-1 isolates, neutralization was due to anti-CD4 antibodies. In these single-chain constructs, the N-termini of CD4D12 and M9 were connected to the C-terminus (residue 511) of gp120 with a long 20-amino acid linker, because the distance between the N-terminus of CD4D12 and the C-terminus of gp120 in the gp120–CD4D12–17b complex [Protein Data Bank (PDB) entry 1G9M] is 45 Å. This long linker might have interrupted the native folding of the molecule and could be responsible for the observed lack of CD4i epitope induction in the gp120-M9 single chain. To overcome this problem, we cyclically permuted gp120 to reduce the linker length and create new N- and C-termini close to the CD4 binding site of the molecule. In circularly permuted proteins, the original N- and C-termini are connected via a peptide linker and new N- and C-termini are created at another position in the sequence. Hence, to circularly permute a protein sequence, the N- and C-termini should be positioned so that they are joined by an amino acid linker and new termini should be created in positions that do not disrupt the folding, stability, or

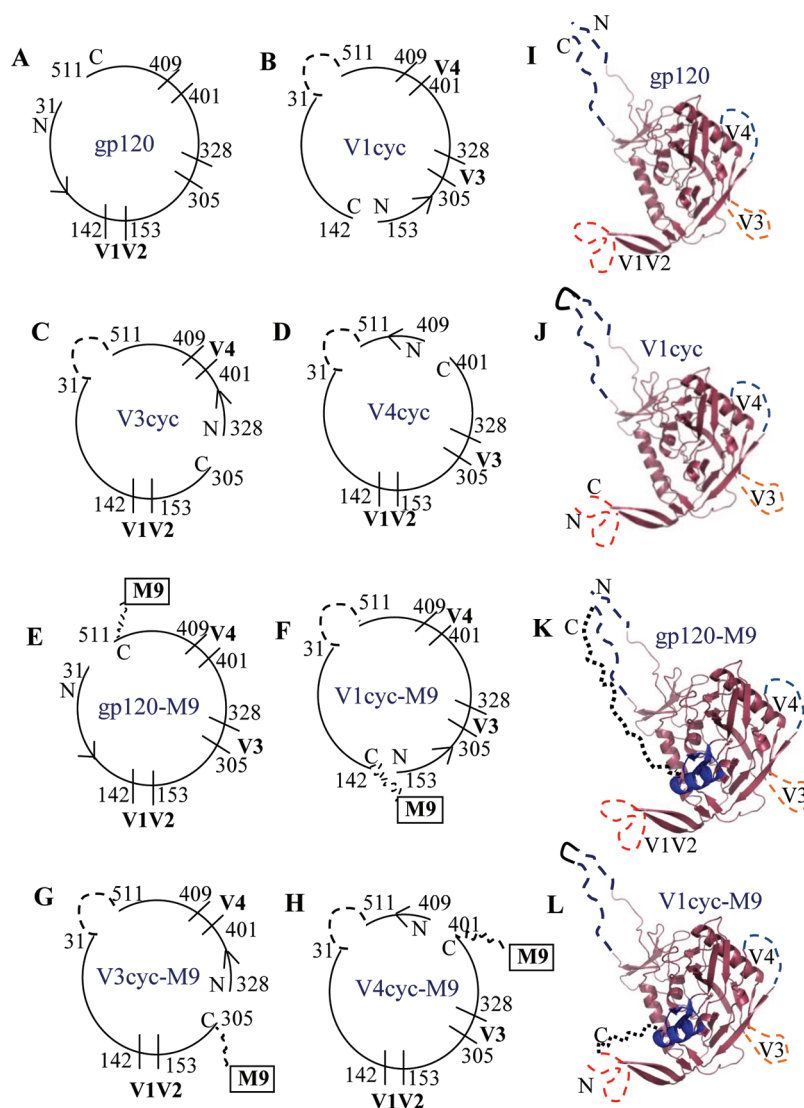


Figure 1. Schematic and cartoon representations of cyclic permutants of gp120 and their single-chain derivatives. Schematic representations of (A) wild-type gp120, (B) V1cyc, (C) V3cyc, (D) V4cyc, (E) gp120-M9, (F) V1cyc-M9, (G) V3cyc-M9, and (H) V4cyc-M9. The numbering of all gp120 constructs follows that of HXBc2. The linker sequence is marked as a dashed line. The amino acid sequence of the linker comprises glycine-serine-alanine repeats. Cartoon diagrams of models of (I) wild-type gp120 (chain G of PDB entry 1YYL), (J) V1cyc, (K) gp120-M9, and (L) V1cyc-M9. gp120 (chain G) is colored light violet, and M33 (chain M, a derivative of M9) is colored blue. The N-terminal (residues 31–82), C-terminal (residues 493–511), V1V2 (residues 128–194), V3 (residues 298–329), and V4 (residues 396–411) regions are shown as long-dash extensions.

biological activity of the permuted molecule. Circular permutation has been well studied for its impact on protein structure, folding, and stability.^{32–42} In the case of gp120, the original N- and C-termini (residues 31 and 511, respectively) were connected by a 20-amino acid linker and new N- and C-termini were created at loops V1, V3, and V4. These are named V1cyc (new N- and C-termini at residues 153 and 142, respectively), V3cyc (new N- and C-termini at residues 328 and 305, respectively), and V4cyc (new N- and C-termini at residues 409 and 401, respectively) (Figure 1). In these cyclic permutants, the loops are completely or partially deleted. For V1cyc, residues from position 143 to 152 were deleted because of poor sequence conservation and the presence of insertions between residues 143 and 144 and residues 150 and 151 in some HIV-1 isolates. For V3cyc, residues 306–327 were deleted. Though the sequence conservation in this region is moderate, there are multiple known insertions between residues 309 and 310, residues 315 and 316, and residues

318 and 319. For V4cyc, residues 402–408 were deleted, because of poor sequence conservation and insertions between residues 406 and 407.

Expression, Purification, and Characterization of Cyclic Permutants of JRFL gp120. The gene sequences of V1cyc, V3cyc, and V4cyc were codon optimized for expression in mammalian cell lines. Plasmid DNAs were transiently transfected into HEK293 cells, and proteins were purified from tissue culture supernatants by affinity chromatography.¹⁰ Yields of purified proteins were approximately 1 mg/L of cell culture supernatant. The gp120 subunit of the envelope binds to cell surface receptor CD4. Following this, conformational changes in gp120 and gp41 occur, ultimately leading to fusion of viral and cellular membranes. To determine whether the cyclic permutants mentioned above are folded into the native conformation, their interaction with four-domain soluble CD4 (sCD4) was measured by SPR. Four-domain sCD4 was immobilized on the surface of a CM5 chip, and different

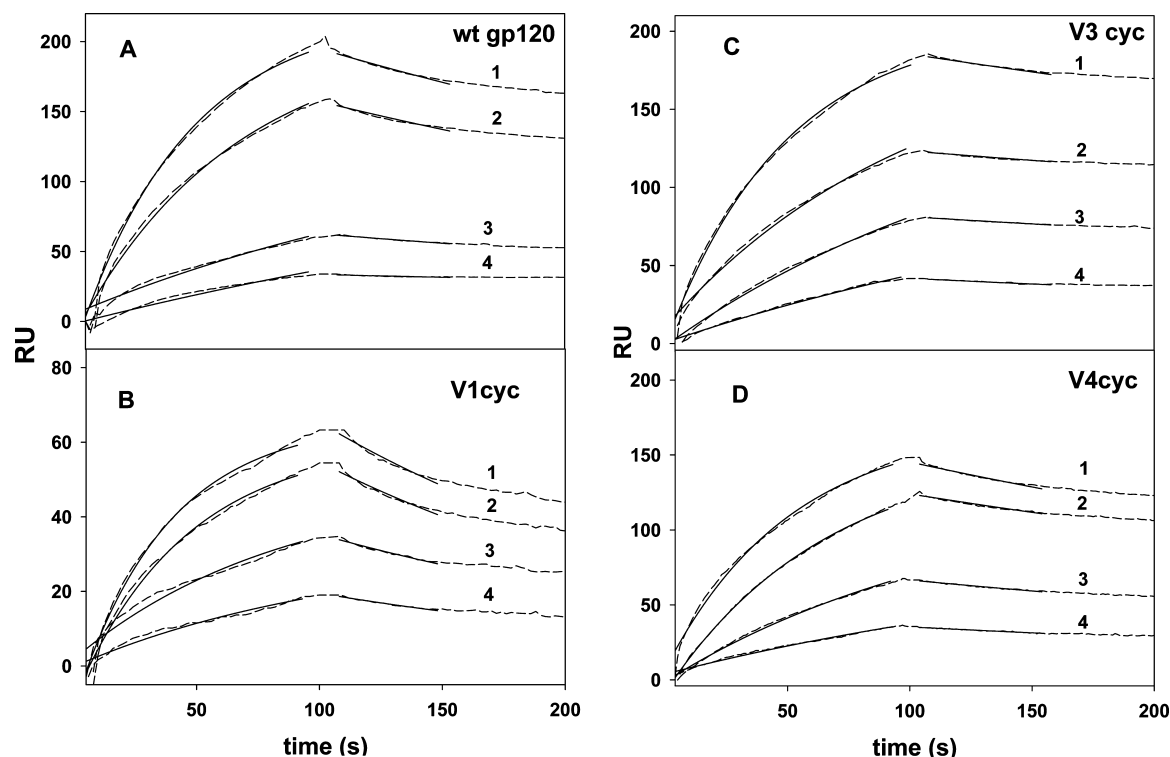


Figure 2. Representative sensorgram overlays for binding of different concentrations of gp120 derivatives to surface-immobilized CD4. Sensorgram overlays are shown as dotted lines, and corresponding fits are shown as solid lines. Each experiment was repeated twice. (A) wt-gp120. Curves 1–4 indicate gp120 concentrations of 75, 50, 25, and 12.5 nM, respectively. (B) V1cyc. Curves 1–4 indicate concentrations of 25.2, 16.6, 8.3, and 4 nM, respectively. (C) V3cyc. Curves 1–4 indicate concentrations of 29.4, 23.2, 11.6, and 5.6 nM, respectively. (D) V4cyc. Curves 1–4 indicate concentrations of 34, 22.4, 11.2, and 5.4 nM, respectively. Surface density of 1000 RU; buffer was PBS (pH 7.4) and 0.005% P20; flow rate of 30 μ L/min.

concentrations of wild-type gp120 and cyclic permutants were passed over the chip surface (Figure 2). Real-time binding to surface-immobilized CD4 was assayed by using the Biacore 2000 SPR instrument. All cyclic permutants bound CD4 with an affinity similar to that of wild-type (wt) gp120 (Table 1). This shows that cyclic permutation of gp120 does not prevent the molecule from folding to the native state.

Table 1. Kinetic Parameters for Binding of wt-gp120 and Its Cyclic Permutants to sCD4

protein	k_{on} ($M^{-1} s^{-1}$)	k_{off} (s^{-1})	K_D (nM)
wt-gp120	1.9×10^5	2.1×10^{-3}	11 ± 2.2
V1cyc	8.7×10^5	5.6×10^{-3}	6.5 ± 0.2
V3cyc	4.9×10^5	1.4×10^{-3}	2.8 ± 0.2
V4cyc	5.1×10^5	2.3×10^{-3}	4.4 ± 0.3
V1cyc-M9	7.19×10^4	2.21×10^{-3}	30.9 ± 4.8
V3cyc-M9	6.63×10^4	1.8×10^{-3}	27 ± 6
h-CMP-V1cyc	1.89×10^6	3.2×10^{-3}	1.7 ± 0.3
SUMO2a-V1cyc	8.7×10^5	4×10^{-3}	4.6 ± 0.1

Construct Design, Expression, Purification, and Characterization of Single-Chain Derivatives of the Cyclic Permutants of gp120. As described above, one of the motivations for making cyclic permutants of gp120 was to fuse these to CD4 analogue M9, to expose CD4i epitopes. To minimize the length of the linker connecting gp120 and M9 in the single-chain derivatives, the N- and C-termini of the cyclic permutants were created near the CD4 binding site (Figure 1). Either the N-terminus of M9 can be connected to the C-

terminus of the cyclic permutant, or the C-terminus of M9 can be connected to the N-terminus of the cyclic permutant by introducing an amino acid linker. The linker length was decided by measuring the distance between the termini of cyclic permutants and M33 from the coordinates of gp120 in complex with M33 and 17b (PDB entry 1YYL).⁴³ V1V2 (residues 128–194) and V3 (residues 298–329) loops have been deleted in the core gp120 construct present in the gp120–M33–17b complex, and residues 396–411 in the V4 loop are disordered. Hence, linker length was decided by measuring the distance between the termini of M33 and the nearest ordered residue of the loop regions in the crystal structure. For V1cyc, the distance between the C-terminus of the cyclic permutant and the N-terminus of M33 (17 Å) was shorter than the distance between the N-terminus of the cyclic permutant and the C-terminus of M33 (27 Å). For V3cyc and V4cyc, both connectivities had similar distances (~ 30 Å), and hence, for both V1 and V3 cyclic permutants, the C-terminus of the cyclic permutant was connected to the N-terminus of M9 with an appropriate linker to generate V1cyc-M9 and V3cyc-M9, respectively. The linker lengths should be 5 and 9 amino acids for V1cyc and V3cyc, respectively (C_{α} – C_{α} distance of 3.8 Å). However, 7- and 12-amino acid linkers were used for V1 and V3 single-chain derivatives, respectively, to ensure the flexibility of the linker. Because V4cyc had linker lengths similar to those of V3cyc, the corresponding single chain with M9 was not constructed. Plasmid DNAs of V1cyc-M9 and V3cyc-M9 were transiently transfected into HEK293 cells, and proteins were purified from tissue culture supernatants by affinity chromatography as described in Experimental Procedures. Yields of purified

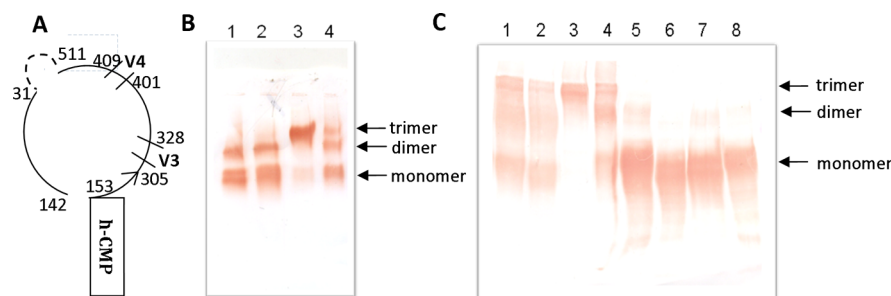


Figure 3. BN-PAGE and SDS-PAGE of monomeric and oligomeric JRFL gp120 derivatives. (A) Schematic representation of h-CMP-V1cyc. (B) 4–12% BN-PAGE, without DTT. wt-gp120, V1cyc, h-CMP-V1cyc, and SUMO2a-V1cyc in lanes 1–4, respectively. (C) 6% SDS-PAGE. Same proteins as in panel B. Lanes 1–4, without DTT; lanes 5–8, with DTT. Following electrophoresis, gels were subjected to Western blotting and probed with rabbit anti-gp120 antisera.

proteins were approximately 1 mg/L of cell culture supernatants. Binding of CD4 to gp120 results in a conformational change in gp120 that exposes cryptic epitopes known as CD4i epitopes. Interaction of mAb 17b with gp120 is considerably enhanced in the presence of CD4; i.e., it binds to CD4i epitopes of gp120.⁴⁴ The binding of both the above gp120-M9 single chain derivatives to 17b, in the presence or absence of sCD4, was characterized by surface plasmon resonance (SPR). 17b was immobilized on the surface of a CM5 chip, and the single-chain derivatives of cyclic permutants with M9 were passed over the chip surface. Real-time binding to surface-immobilized 17b was assayed using the Biacore 2000 SPR instrument.

Binding was assayed both in the presence and in the absence of a 5-fold excess of soluble CD4. Neither V1cyc-M9 nor V3cyc-M9 interacted with 17b in the absence of sCD4; i.e., reduction of the linker length did not help in exposing the CD4-induced cryptic epitopes. Even in the presence of sCD4, these single-chain derivatives did not bind 17b, which implies that the coreceptor binding sites are either not exposed or partially occluded by M9. Unexpectedly, these single-chain derivatives bound surface-immobilized sCD4 with a slightly lower affinity than the corresponding cyclic permutants, probably because of the partial occupancy of M9 in the CD4 binding site (Table 1).

Design of Trimeric Derivatives of Cyclically Permuted JRFL gp120. Recently, a cryo-electron density map of HIV-1 env (BAL isolate) on the virion surface was obtained.²² After the crystal structures of monomeric core gp120 in complex with b12 (PDB entry 2NY7) had been fit into the electron density map, it was found that there was excess electron density at the trimer interface that was attributed to the V1V2 loops. On the basis of this observation, we hypothesized that insertion of a heterologous trimerization sequence into this region might help in the formation of native-like trimers that present loop-derived neutralization epitopes. Most trimerization domains and especially trimeric coiled coils⁴⁵ have large distances between the N- and C-termini, making them unsuitable for insertion into loop regions of a protein. In an alternative approach, we have individually fused two different trimerization domains at the N-terminus of V1cyc. A schematic of one of the trimerization domains fused to V1cyc is shown in Figure 3A.

The trimerization domain of human cartilage matrix protein (h-CMP) is a trimeric coiled coil with two cysteine residues N-terminal to the coiled coil that form interchain disulfide bonds. The NMR structure of the homologue from chicken (CCMP) has been determined,⁴⁶ and the CCMP trimerization domain

has previously been used for trimerization of gp140.⁴⁷ In our study, we used the human homologue of the trimerization sequence. In addition, we also used another trimerization domain from the human SUMO2 protein.²⁹ The structure was analyzed using MODIP⁴⁸ to predict possible locations for the introduction of intersubunit disulfides into SUMO2 with the aim of generating disulfide-linked trimers. On the basis of MODIP predictions, mutations D26C and A46C were introduced. Both proteins were purified from HEK293 cells by affinity chromatography. BN-PAGE analysis, followed by Western blotting, showed that h-CMP-V1cyc exists mainly as a trimer and SUMO2a-V1cyc is a mixture of a trimer, a dimer, and a monomer (Figure 3B). SDS-PAGE analysis, followed by Western blotting in the presence and absence of DTT, showed that both constructs form disulfide-linked oligomers (Figure 3C).

Interaction of Trimers with sCD4. Binding of the h-CMP and SUMO2a gp120 fusion proteins to surface-immobilized sCD4 was assessed using SPR (Figure 4). h-CMP and SUMO2a fusions bound to sCD4 with ~6- and 2.5-fold higher affinity than wt-gp120 (Table 1). The enhanced binding was primarily due to the increased k_{on} . The lower affinity of SUMO2a fusion protein for sCD4, compared to that of h-CMP fusion protein, probably results from a smaller amount of formation of trimer in the former protein under native conditions.

Interaction of Trimers with CD4 Binding Site Antibodies b12 and F105. Broadly neutralizing antibody b12 interacts with gp120 at the junction of the proximal and distal barrels of the outer domain and blocks CD4 binding.⁴⁹ F105 is a non-neutralizing CD4 binding site (CD4bs) antibody that also binds in a region of gp120 that partially overlaps with b12. While this binds more tightly than b12 to monomeric gp120, unlike b12 they do not bind to the native env trimer on the virion surface. Upon interaction with b12, gp120 on the trimeric envelope spike is locked in a conformation, which prevents further conformational changes for interaction with cell surface receptor CD4.²² In contrast to monomeric gp120, h-CMP-V1cyc interacted with similar affinities of ~10 nM to both the broadly neutralizing antibody b12 and non-neutralizing antibody F105 (Table 2). SUMO2a-V1cyc binds approximately 5–10-fold weaker than gp120 to b12 and F105 (Table 2). The improved binding of the h-CMP derivative is consistent with its fully trimeric association and is probably caused by avidity effects.

Monomeric and both trimeric versions of V1cyc bound less well to F105 than wt-gp120 (Table 2). F105 interacts with the

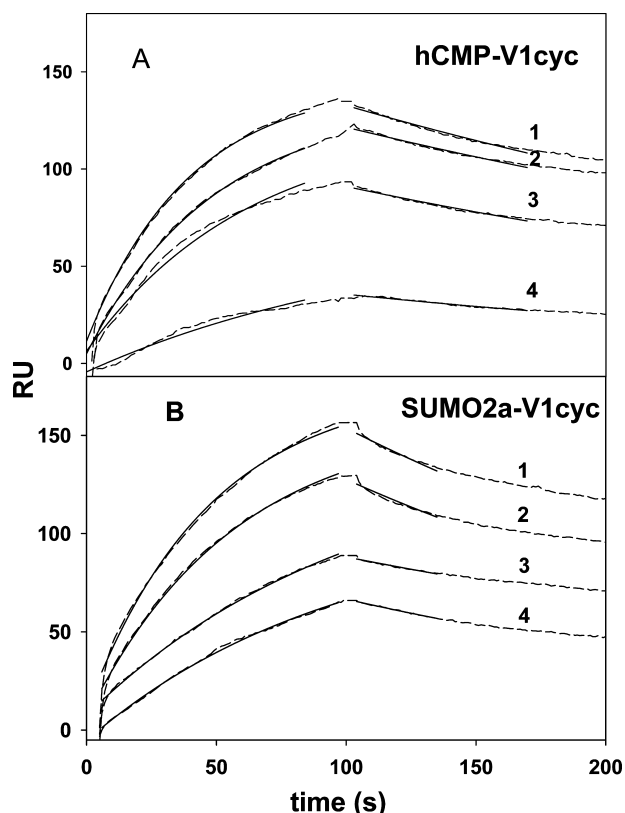


Figure 4. Representative sensorgram overlays for binding of different concentrations of trimerized gp120 derivatives to surface-immobilized CD4. Sensorgram overlays are shown as dotted lines and corresponding fits as solid lines. Each experiment was repeated twice. (A) Binding of h-CMP-V1cyc. Curves 1–4 indicate concentrations of 8, 6, 4, and 2 nM, respectively. (B) Binding of SUMO2a-V1cyc. Curves 1–4 indicate concentrations of 8, 6, 4, and 2 nM, respectively. Surface density of 1000 RU; buffer was PBS (pH 7.4) and 0.005% P20; flow rate of 30 μ L/min.

Table 2. Kinetic Parameters of Binding of h-CMP-V1cyc and SUMO2a-V1cyc to Neutralizing Antibody b12 and Non-Neutralizing Antibody F105

antibody	construct	k_{on} ($M^{-1} s^{-1}$)	k_{off} (s^{-1})	K_D (nM)
b12	wt-gp120	8.5×10^4	2×10^{-3}	23 ± 1.3
	V1cyc	1.9×10^5	9.5×10^{-3}	51 ± 2.6
	h-CMP-V1cyc	8.9×10^4	6.5×10^{-4}	7.3 ± 2.3
	SUMO2a-V1cyc	2.4×10^4	5.6×10^{-3}	230 ± 25
F105	wt-gp120	7.5×10^4	1.9×10^{-4}	2.5 ± 1.1
	V1cyc	4.3×10^5	3.4×10^{-3}	7.9 ± 0.5
	h-CMP-V1cyc	1.4×10^5	1.4×10^{-3}	10 ± 2.7
	SUMO2a-V1cyc	6.7×10^4	1.0×10^{-3}	15 ± 4.4

hydrophobic surface of gp120 near the bridging sheet.⁵⁰ Bridging sheet strands β 20 and β 21 and strands β 2 and β 3 move apart to facilitate this interaction. The presence of the covalently linked trimerization domains at the top of the V1 loop (that emanated from strands β 2 and β 3) may inhibit the movement of the bridging sheet strands required for F105 interaction.

Design of Cyclic Permutants of gp120 To Improve the Affinity for PG9 and PG16. While this work was in progress, Walker et al. reported the isolation of two broadly neutralizing antibodies, PG9 and PG16, from an African donor.⁵¹ PG9 and PG16 were able to neutralize \sim 80% of the HIV-1 isolates from

different clades. These two antibodies were able to recognize gp120 on the virion surface but interacted weakly with recombinant gp120 from most HIV-1 isolates. Although PG9 and PG16 were able to neutralize many HIV-1 isolates, they did not neutralize JRFL but bound and neutralized the closely related JRCSF virus. However, introduction of the E168K mutation into JRFL rendered it sensitive to neutralization by these mAbs.⁵¹ However, introduction of the E168K mutation into h-CMP-V1cyc did not lead to PG9 or PG16 binding (data not shown).

Mutational analyses indicated that the PG9 and PG16 epitopes contain residues in the V1V2 and V3 loops.⁵¹ In case of V1cyc, \sim 10 residues were deleted from the V1 loop. Because these residues may play an important role in the proper folding of the loop and antibody binding, two more cyclic permutants were designed without deletions in the V1 and V2 loops. h-CMP was used as the trimerization domain in these constructs. The cyclic permutants were h-CMP-V1cyc1 (new N- and C-termini at residues 144 and 142, respectively; h-CMP is fused at the N-terminus of the putative apex of the V1 loop) and V2cyc-h-CMP (new N- and C-termini at residues 177 and 176, respectively; h-CMP is fused at the C-terminus of the putative apex of the V2 loop). These two constructs were based on the JRCSF gp120 sequence.

Purification and Characterization of wt-JRCSF gp120, h-CMP-V1cyc1, and V2cyc-h-CMP. Plasmid DNAs of all three constructs were transiently transfected in HEK293 cells, and proteins were purified using affinity chromatography. BN-PAGE analysis followed by Western blotting showed that h-CMP-V1cyc1 exists mainly as a trimer and V2cyc-h-CMP is a mixture of a trimer, a dimer, and a monomer (Figure 5A). SDS-PAGE followed by Western blotting in the presence and absence of DTT showed that both constructs form disulfide-linked oligomers (Figure 5B). Binding to PG9 and PG16 was characterized using SPR (Figure 6). h-CMP-V1cyc1 bound PG9 and PG16 with \sim 20-fold higher affinity than wild-type JRCSF gp120 (Table 3). However, V2cyc-h-CMP did not show any interaction with PG9 or PG16. This is probably because residues 173–176 are very important for PG9 and PG16 binding, and the epitope is disrupted by cleavage between residues 176 and 177. Additionally, this region may point away from the trimer interface.

DISCUSSION

Despite intensive efforts, discovery of an immunogen eliciting broadly neutralizing antibodies against HIV-1 remains elusive. Most potent broadly neutralizing antibodies, against HIV-1, target conserved regions on the gp120 surface subunit of the env protein.^{51–53} The virus has evolved multiple strategies of immune evasion, such as glycosylation of conserved regions, a high degree of sequence variation, and conformational flexibility. In addition to the CD4 binding site, another conserved region in gp120 is the coreceptor binding site. Cryptic epitopes in this region show increased levels of exposure after CD4 binding. As discussed above, a previous gp120-M9 single chain¹⁰ did not display the desired CD4i epitopes or elicit neutralizing antibodies. To reduce the length of the linker joining gp120 and M9, in this study, gp120 was cyclically permuted and new N- and C-termini were created within the V1, V3, and V4 loop regions. The cyclic permutants were able to bind sCD4 with an affinity similar to that of wild-type gp120, indicating they are properly folded. Unfortunately, single-chain derivatives of these cyclic permutants and M9 did

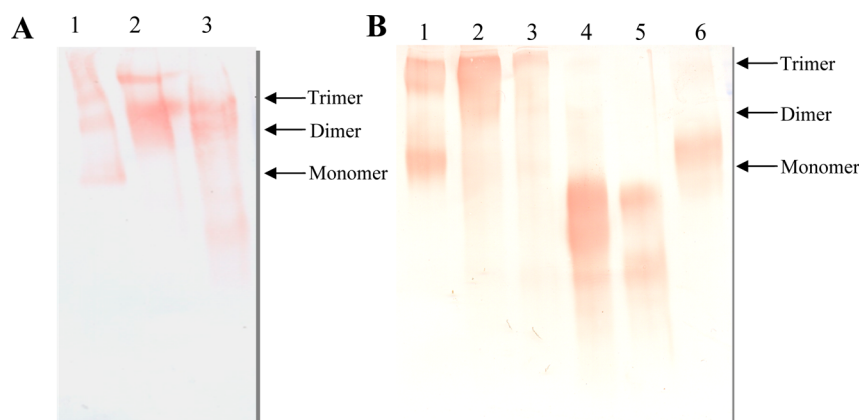


Figure 5. BN-PAGE and SDS-PAGE analysis of monomeric and oligomeric JRCSF gp120 derivatives. (A) 4–12% BN-PAGE, without DTT. JRCSF gp120, h-CMP-V1cyc1, and V2cyc-h-CMP in lanes 1–3, respectively. (B) 6% SDS-PAGE. JRCSF gp120, h-CMP-V1cyc1, and V2cyc-h-CMP in lanes 1–3, respectively, without DTT; h-CMP-V1cyc1, V2cyc-h-CMP, and JRCSF gp120 in lanes 4–6, respectively, with DTT. Following electrophoresis, gels were subjected to Western blotting and probed with rabbit anti-gp120 antisera.

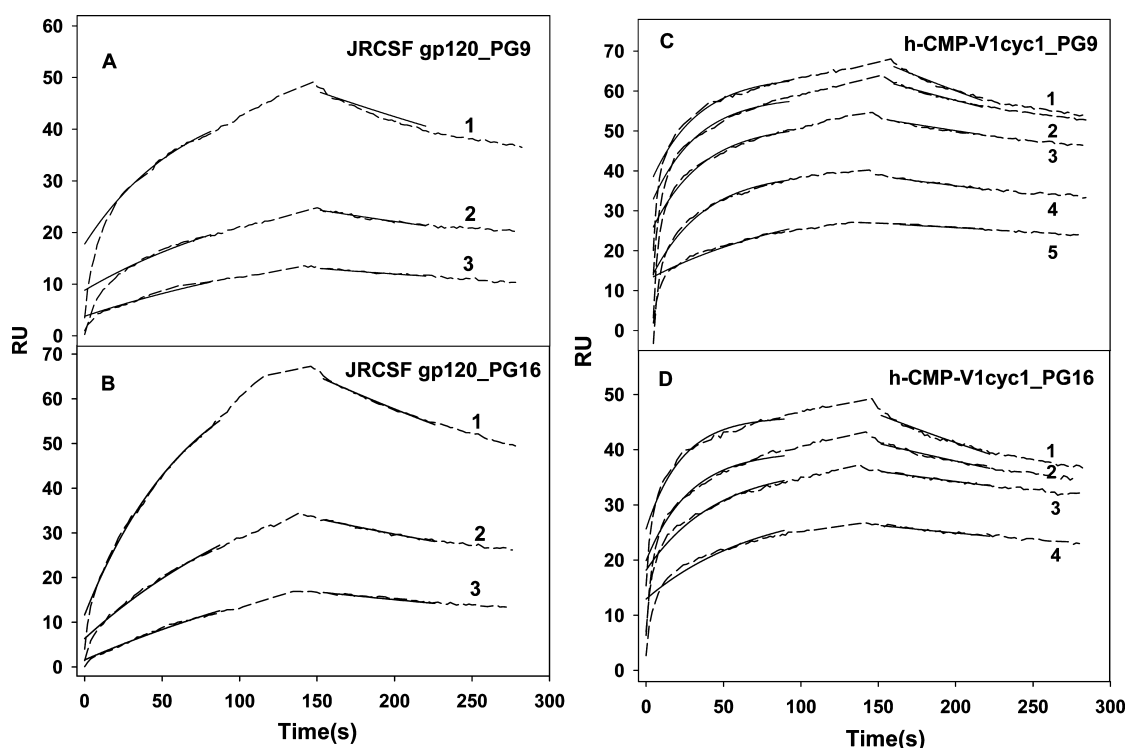


Figure 6. Representative sensorgram overlays of binding of different concentrations of JRCSF gp120 and h-CMP-V1cyc1 to immobilized PG9 and PG16. Sensorgram overlays are shown as dotted lines and corresponding fits as solid lines. Each experiment was repeated twice. (A) Binding of JRCSFgp120 to surface-immobilized PG9. Curves 1–3 indicate concentrations of 1.6, 0.83, and 0.41 μM , respectively. (B) Binding of JRCSF gp120 to surface-immobilized PG16. Curves 1–3 indicate concentrations of 1.6, 0.83, and 0.41 μM , respectively. (C) Binding of h-CMP-V1cyc1 to surface-immobilized PG9. Curves 1–5 indicate concentrations of 2.55, 1.66, 0.8, 0.41, and 0.208 μM , respectively. (D) Binding of h-CMP-V1cyc1 to surface-immobilized PG16. Curves 1–4 indicate concentrations of 2.55, 1.66, 0.8, and 0.41 μM , respectively. Surface density of 1500 RU; buffer of PBS (pH 7.4) and 0.005% P20; flow rate of 20 $\mu\text{L}/\text{min}$.

Table 3. Kinetic Parameters for Binding of JRCSFgp120 and h-CMP-V1cyc1 to Broadly Neutralizing Antibodies PG9 and PG16

antibody	construct	k_{on} ($\text{M}^{-1} \text{s}^{-1}$)	k_{off} (s^{-1})	K_{D} (nM)
PG9	JRCSF gp120	1.9×10^4	2.3×10^{-3}	123 ± 14
	h-CMP-V1cyc1	1.7×10^5	1.3×10^{-3}	7.6 ± 1.2
PG16	JRCSF gp120	1.0×10^4	2.2×10^{-3}	200 ± 17
	h-CMP-V1cyc1	8.8×10^4	1.6×10^{-3}	17 ± 16

not interact strongly with 17b. Thus, even with a reduced linker length, the currently designed cycgp120-M9 single chains do not display the desired CD4i epitopes. In a recent study, gp120 and a synthetic CD4 mimic M64U-1 were cross-linked via a disulfide exchange reaction to expose CD4i epitopes.⁵⁴ Although these cross-linked constructs were able to interact with 17b and 48d, when used as an immunogen they did not elicit broadly neutralizing antibodies. This suggests that CD4i epitopes are not a good target for immunogen design, possibly

because they are only accessible for a brief period after CD4 binding.

Most neutralizing antibodies target epitopes on gp120 that are exposed on the native virion env spike. On the basis of a previous model of the HIV-1 spike derived from cryo-electron tomography, in this work we have fused two different trimerization domains at the putative tip of the V1V2 loop. In contrast to previous studies, where trimerization domains were added at the C-terminus of gp140, gp130, and gp120, here we have used the cyclic permutant V1cyc to incorporate the trimerization domains. h-CMP-V1cyc formed a covalently linked trimer, whereas SUMO2a-V1cyc was a mixture of a trimer, a dimer, and a monomer. Previous trimeric gp140 constructs (gp140–GCN4 and gp140–fibrin)¹⁴ were characterized for antibody binding. These showed ~1.5-fold better binding to neutralizing antibodies b12 and 2G12 than monomeric gp120, while binding to non-neutralizing antibodies (F105 and F91) was 2-fold weaker. Similar efforts in the context of gp120, however, showed that monomeric gp120 and the gp120–GCN4 trimer bound CD4, b12, and F105 similarly in enzyme-linked immunosorbent assays.¹⁵ In our work, the h-CMP trimer bound sCD4 and b12 ~5- and 3-fold better than monomeric gp120. Both h-CMP- and SUMO2a-fused V1cyc bound non-neutralizing antibody F105 ~4-fold worse than wt-gp120, suggesting that these constructs might more closely mimic the native trimeric spike than earlier trimeric constructs. Overall, in this work, it has been shown that V1 cyclic permutants of gp120 with an appropriate trimerization domain can fold into a conformation that shows improved affinity for neutralizing antibody b12 and poorer affinity for non-neutralizing CD4bs antibody F105 relative to gp120. We have also shown that cyclic permutants of monomeric gp120 in the V1, V3, or V4 region are all competent to fold and to bind CD4. These cyclic permutants with altered chain connectivity can serve as the basis for future gp120 derivatives.

Cryo-electron tomography has suggested that the env trimer is stabilized at the membrane proximal region by gp41 and at the membrane distal apex by V1V2 loops. In contrast to previous studies, where gp120 trimers were stabilized by using trimerization domains at the bottom (membrane proximal region) of the spike, in this study, we have used a V1 cyclic permutant to stabilize the trimer by holding it together at the proposed apex of the spike.

Because JRFL env does not bind to PG9 or PG16,⁵¹ new cyclic permutants were made on the basis of the JRCSF sequence that contained all residues in the V1V2 loop. New N- and C-termini were generated either at the putative tip of the V1 or at the putative tip of the V2 loop. h-CMP was added at the N-terminus of V1cyc1 and the C-terminus of V2cyc. h-CMP-V1cyc1 bound PG9 and PG16 with ~20-fold higher affinity than JRCSF wt-gp120. V2cyc-h-CMP did not show any interaction with PG9 or PG16. It is known from mutagenesis studies that residues 173, 176, and 177 are important for binding to PG9 and PG16. PG16 is known to interact via its unusually long (28-residue) CDRH3 domain. It may be that the presence of the trimerization domain near these residues has sterically blocked access of these broadly neutralizing antibodies to the protein and/or this region of the V2 loop points away from the trimer interface. While this work was in progress, the crystal structure of the V1V2 domain of gp120 in complex with broadly neutralizing antibody PG9 was determined.⁵⁵ The structure showed that residues 142–144 are in a loop region distant from the binding site of PG9. This

is consistent with the observed sequence variability in this region and validates our choices of residues for cyclic permutation in V1cyc and V1cyc1. However, residues 176 and 177 are in a β -strand region that largely contains an important component of the PG9 epitope. Hence, insertion of a trimerization domain into the middle of a strand in the case of V2cyc-h-CMP is expected to disrupt the epitope, consistent with the lack of PG9 or PG16 binding seen for h-CMP-V2cyc.

There are several proposed models for the native HIV-1 env trimer that have been derived from cryo-electron microscopy and tomography studies.^{22–26} These models differ from one another in several aspects. In some, the membrane proximal region forms a single stalk,^{22,24,26} while in others, it appears to be a tripod.^{23,25} The V1 and V2 regions are located far from the trimer axis in some models^{23,24,26} and close to it in others^{22,25} and can be either membrane proximal^{23,26} or distal.^{22,25}

This work shows that gp120 can be circularly permuted at multiple locations without its native fold and activity being affected. The resulting constructs can be trimerized by adding trimerization domains to either their N- or C-termini. This work also shows that insertion of a trimerization domain into the V1 loop enhances binding of both PG9 and PG16 to gp120. This strongly suggests that the V1 loop is proximal to the trimer interface in native env, consistent with the location of the V1V2 loop suggested in ref 22 (Figure 7). If this were not

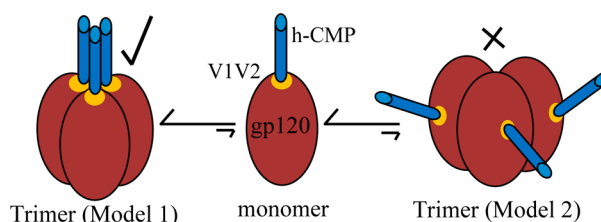


Figure 7. Schematic description of h-CMP (blue) fused to cyclically permuted gp120 (dark red). The yellow region marks the location of the V1V2 loop region of gp120. If the V1V2 regions are near the apex of the native, trimeric spike (model 1), then in h-CMP-V1cyc the equilibrium should be shifted toward the trimer. On the other hand, if the V1V2 loops are located far from the trimer axis (model 2), the equilibrium in h-CMP-V1cyc should be shifted toward the monomer. The data support model 1.

the case, insertion of the trimerization domain would have led to a large distortion in the relative orientations of V1V2 and V3 loops in each monomer and a consequent loss of PG9 and PG16 binding.

Addition of trimerization domains at the V1 loop of cyclic permutants of gp120 resulted in the formation of predominantly trimeric species, which bound CD4 and neutralizing antibodies b12, PG9, and PG16 with higher affinity but bound non-neutralizing antibody F105 with lower affinity than wild-type monomeric gp120. Such trimeric constructs may be useful as potential immunogens as well as in probing and characterizing binding sites for recently discovered, highly potent broadly neutralizing antibodies.⁵² Results from the recent RV144 vaccine trial^{56,57} suggested a role for V2 binding antibodies in vaccine-mediated protection. This further emphasizes the importance of immunogens that appropriately display this region of the env protein.

AUTHOR INFORMATION

Corresponding Author

*Molecular Biophysics Unit, Indian Institute of Science, Bangalore 560 012, India. Telephone: 91-80-22932612. Fax: 91-80-23600535. E-mail: varadar@mbu.iisc.ernet.in.

Author Contributions

P.S., S.B., and S.K. contributed equally to this work.

Funding

[†]This work was supported by grants from the Department of Biotechnology, Government of India, to R.V., P.S., and S.B. and S.K. are recipients of fellowships from the Council of Scientific and Industrial Research, Government of India.

Notes

The authors declare no competing financial interest.

ACKNOWLEDGMENTS

Antibody b12 was obtained from the Neutralizing Antibody Consortium. Antibody F105 was provided by Dr. L. Cavacini. sCD4 was obtained from the AIDS Research and Reference Reagent program. We thank Dr. S. Phogat for helpful discussions and for providing antibodies PG9 and PG16.

ABBREVIATIONS

CD4bs, CD4 binding site; h-CMP, human cartilage matrix protein; wt-gp120, wild-type gp120; env, envelope; CD4i, CD4-induced; CD4D12, two-domain CD4; BCA, bicinchoninic acid; BN-PAGE, blue native-PAGE; SDS-PAGE, sodium dodecyl sulfate-polyacrylamide gel electrophoresis; MOPS, 3-(N-morpholino)propanesulfonic acid; RU, resonance units; sCD4, four-domain soluble CD4; SPR, surface plasmon resonance; CCMP, chicken cartilage matrix protein; CDRH3, complementarity-determining region in the third heavy chain; V1cyc, cyclically permuted gp120 with new N- and C-termini at residues 153 and 142, respectively; V3cyc, cyclically permuted gp120 with new N- and C-termini at residues 328 and 305, respectively; V4cyc, cyclically permuted gp120 with new N- and C-termini at residues 409 and 401, respectively; V1cyc-M9, M9 fused at the C-terminus of V1cyc; V3cyc-M9, M9 fused at the C-terminus of V3cyc; h-CMP-V1cyc, h-CMP fused at the N-terminus of V1cyc; SUMO2a-V1cyc, SUMO2a fused at the N-terminus of V1cyc; h-CMP-V1cyc1, h-CMP fused at the N-terminus of cyclically permuted gp120 with new N- and C-termini at residues 144 and 142, respectively; h-CMP-V2cyc, h-CMP fused at the N-terminus of cyclically permuted gp120 with new N- and C-termini at residues 177 and 176, respectively.

REFERENCES

- (1) Parren, P. W., Gauduin, M. C., Koup, R. A., Poignard, P., Fiscaro, P., Burton, D. R., and Sattentau, Q. J. (1997) Relevance of the antibody response against human immunodeficiency virus type 1 envelope to vaccine design. *Immunol. Lett.* 57, 105–112.
- (2) Wyatt, R., and Sodroski, J. (1998) The HIV-1 envelope glycoproteins: Fusogens, antigens, and immunogens. *Science* 280, 1884–1888.
- (3) Kwong, P. D., Wyatt, R., Robinson, J., Sweet, R. W., Sodroski, J., and Hendrickson, W. A. (1998) Structure of an HIV gp120 envelope glycoprotein in complex with the CD4 receptor and a neutralizing human antibody. *Nature* 393, 648–659.
- (4) Schultz, A. M., and Bradac, J. A. (2001) The HIV vaccine pipeline, from preclinical to phase III. *AIDS* 15 (Suppl. 5), S147–S158.

- (5) Celada, F., Cambiaggi, C., Maccari, J., Burastero, S., Gregory, T., Patzer, E., Porter, J., McDanal, C., and Matthews, T. (1990) Antibody raised against soluble CD4-gp120 complex recognizes the CD4 moiety and blocks membrane fusion without inhibiting CD4-gp120 binding. *J. Exp. Med.* 172, 1143–1150.
- (6) Kang, C. Y., Hariharan, K., Nara, P. L., Sodroski, J., and Moore, J. P. (1994) Immunization with a soluble CD4-gp120 complex preferentially induces neutralizing anti-human immunodeficiency virus type 1 antibodies directed to conformation-dependent epitopes of gp120. *J. Virol.* 68, 5854–5862.
- (7) Devico, A., Silver, A., Thronton, A. M., Sarngadharan, M. G., and Pal, R. (1996) Covalently crosslinked complexes of human immunodeficiency virus type 1 (HIV-1) gp120 and CD4 receptor elicit a neutralizing immune response that includes antibodies selective for primary virus isolates. *Virology* 218, 258–263.
- (8) Fouts, T., Godfrey, K., Bobb, K., Montefiori, D., Hanson, C. V., Kalyanaraman, V. S., DeVico, A., and Pal, R. (2002) Crosslinked HIV-1 envelope-CD4 receptor complexes elicit broadly cross-reactive neutralizing antibodies in rhesus macaques. *Proc. Natl. Acad. Sci. U.S.A.* 99, 11842–11847.
- (9) DeVico, A., Fouts, T., Lewis, G. K., Gallo, R. C., Godfrey, K., Charurat, M., Harris, L., Galmin, L., and Pal, R. (2007) Antibodies to CD4-induced sites in HIV gp120 correlate with the control of SHIV challenge in macaques vaccinated with subunit immunogens. *Proc. Natl. Acad. Sci. U.S.A.* 104, 17477–17482.
- (10) Varadarajan, R., Sharma, D., Chakraborty, K., Patel, M., Citron, M., Sinha, P., Yadav, R., Rashid, U., Kennedy, S., Eckert, D., Geleziunas, R., Bramhill, D., Schleif, W., Liang, X., and Shiver, J. (2005) Characterization of gp120 and its single-chain derivatives, gp120-CD4D12 and gp120-M9: Implications for targeting the CD4i epitope in human immunodeficiency virus vaccine design. *J. Virol.* 79, 1713–1723.
- (11) Binley, J. M., Sanders, R. W., Clas, B., Schuelke, N., Master, A., Guo, Y., Kajumo, F., Anselma, D. J., Maddon, P. J., Olson, W. C., and Moore, J. P. (2000) A recombinant human immunodeficiency virus type 1 envelope glycoprotein complex stabilized by an intermolecular disulfide bond between the gp120 and gp41 subunits is an antigenic mimic of the trimeric virion-associated structure. *J. Virol.* 74, 627–643.
- (12) Sanders, R. W., Vesanan, M., Schuelke, N., Master, A., Schiffer, L., Kalyanaraman, R., Paluch, M., Berkhout, B., Maddon, P. J., Olson, W. C., Lu, M., and Moore, J. P. (2002) Stabilization of the soluble, cleaved, trimeric form of the envelope glycoprotein complex of human immunodeficiency virus type 1. *J. Virol.* 76, 8875–8889.
- (13) Schulke, N., Vesanan, M. S., Sanders, R. W., Zhu, P., Lu, M., Anselma, D. J., Villa, A. R., Parren, P. W., Binley, J. M., Roux, K. H., Maddon, P. J., Moore, J. P., and Olson, W. C. (2002) Oligomeric and conformational properties of a proteolytically mature, disulfide-stabilized human immunodeficiency virus type 1 gp140 envelope glycoprotein. *J. Virol.* 76, 7760–7776.
- (14) Yang, X., Lee, J., Mahony, E. M., Kwong, P. D., Wyatt, R., and Sodroski, J. (2002) Highly stable trimers formed by human immunodeficiency virus type 1 envelope glycoproteins fused with the trimeric motif of T4 bacteriophage fibrin. *J. Virol.* 76, 4634–4642.
- (15) Pancera, M., Lebowitz, J., Schon, A., Zhu, P., Freire, E., Kwong, P. D., Roux, K. H., Sodroski, J., and Wyatt, R. (2005) Soluble mimetics of human immunodeficiency virus type 1 viral spikes produced by replacement of the native trimerization domain with a heterologous trimerization motif: Characterization and ligand binding analysis. *J. Virol.* 79, 9954–9969.
- (16) Center, R. J., Lebowitz, J., Leapman, R. D., and Moss, B. (2004) Promoting trimerization of soluble human immunodeficiency virus type 1 (HIV-1) Env through the use of HIV-1/simian immunodeficiency virus chimeras. *J. Virol.* 78, 2265–2276.
- (17) Farzan, M., Choe, H., Desjardins, E., Sun, Y., Kuhn, J., Cao, J., Archambault, D., Kolchinsky, P., Koch, M., Wyatt, R., and Sodroski, J. (1998) Stabilization of human immunodeficiency virus type 1 envelope glycoprotein trimers by disulfide bonds introduced into the gp41 glycoprotein ectodomain. *J. Virol.* 72, 7620–7625.

- (18) Yang, X., Farzan, M., Wyatt, R., and Sodroski, J. (2000) Characterization of stable, soluble trimers containing complete ectodomains of human immunodeficiency virus type 1 envelope glycoproteins. *J. Virol.* 74, 5716–5725.
- (19) Yang, X., Florin, L., Farzan, M., Kolchinsky, P., Kwong, P. D., Sodroski, J., and Wyatt, R. (2000) Modifications that stabilize human immunodeficiency virus envelope glycoprotein trimers in solution. *J. Virol.* 74, 4746–4754.
- (20) Yang, X., Wyatt, R., and Sodroski, J. (2001) Improved elicitation of neutralizing antibodies against primary human immunodeficiency viruses by soluble stabilized envelope glycoprotein trimers. *J. Virol.* 75, 1165–1171.
- (21) Pancera, M., and Wyatt, R. (2005) Selective recognition of oligomeric HIV-1 primary isolate envelope glycoproteins by potentially neutralizing ligands requires efficient precursor cleavage. *Virology* 332, 145–156.
- (22) Liu, J., Bartsaghi, A., Borgnia, M. J., Sapiro, G., and Subramaniam, S. (2008) Molecular architecture of native HIV-1 gp120 trimers. *Nature* 455, 109–113.
- (23) Zhu, P., Liu, J., Bess, J. Jr., Chertova, E., Lifson, J. D., Grise, H., Ofek, G. A., Taylor, K. A., and Roux, K. H. (2006) Distribution and three-dimensional structure of AIDS virus envelope spikes. *Nature* 441, 847–852.
- (24) Zanetti, G., Briggs, J. A., Grunewald, K., Sattentau, Q. J., and Fuller, S. D. (2006) Cryo-electron tomographic structure of an immunodeficiency virus envelope complex in situ. *PLoS Pathog.* 2, e83.
- (25) Wu, S. R., Loving, R., Lindqvist, B., Hebert, H., Koeck, P. J., Sjöberg, M., and Garoff, H. (2010) Single-particle cryoelectron microscopy analysis reveals the HIV-1 spike as a tripod structure. *Proc. Natl. Acad. Sci. U.S.A.* 107, 18844–18849.
- (26) Moscoso, C. G., Sun, Y., Poon, S., Xing, L., Kan, E., Martin, L., Green, D., Lin, F., Vahlne, A. G., Barnett, S., Srivastava, I., and Cheng, R. H. (2011) Quaternary structures of HIV Env immunogen exhibit conformational vicissitudes and interface diminution elicited by ligand binding. *Proc. Natl. Acad. Sci. U.S.A.* 108, 6091–6096.
- (27) Vita, C., Drakopoulou, E., Vizzavona, J., Rochette, S., Martin, L., Menez, A., Roumestand, C., Yang, Y. S., Ylisastigui, L., Benjouad, A., and Gluckman, J. C. (1999) Rational engineering of a miniprotein that reproduces the core of the CD4 site interacting with HIV-1 envelope glycoprotein. *Proc. Natl. Acad. Sci. U.S.A.* 96, 13091–13096.
- (28) Jenkins, R. N., Osborne-Lawrence, S. L., Sinclair, A. K., Eddy, R. L. Jr., Byers, M. G., Shows, T. B., and Duby, A. D. (1990) Structure and chromosomal location of the human gene encoding cartilage matrix protein. *J. Biol. Chem.* 265, 19624–19631.
- (29) Huang, W. C., Ko, T. P., Li, S. S., and Wang, A. H. (2004) Crystal structures of the human SUMO-2 protein at 1.6 and 1.2 Å resolution: Implication on the functional differences of SUMO proteins. *Eur. J. Biochem.* 271, 4114–4122.
- (30) Bajaj, K., Dewan, P. C., Chakrabarti, P., Goswami, D., Barua, B., Baliga, C., and Varadarajan, R. (2008) Structural correlates of the temperature sensitive phenotype derived from saturation mutagenesis studies of CcdB. *Biochemistry* 47, 12964–12973.
- (31) Bhattacharyya, S., Rajan, R. E., Swarupa, Y., Rathore, U., Verma, A., Udaykumar, R., and Varadarajan, R. (2010) Design of a non-glycosylated outer domain-derived HIV-1 gp120 immunogen that binds to CD4 and induces neutralizing antibodies. *J. Biol. Chem.* 285, 27100–27110.
- (32) Buchwalder, A., Szadkowski, H., and Kirschner, K. (1992) A fully active variant of dihydrofolate reductase with a circularly permuted sequence. *Biochemistry* 31, 1621–1630.
- (33) Pollard, S. R., Rosa, M. D., Rosa, J. J., and Wiley, D. C. (1992) Truncated variants of gp120 bind CD4 with high affinity and suggest a minimum CD4 binding region. *EMBO J.* 11, 585–591.
- (34) Yang, Y. R., and Schachman, H. K. (1993) Aspartate transcarbamoylase containing circularly permuted catalytic polypeptide chains. *Proc. Natl. Acad. Sci. U.S.A.* 90, 11980–11984.
- (35) Zhang, T., Bertelsen, E., Benvegna, D., and Alber, T. (1993) Circular permutation of T4 lysozyme. *Biochemistry* 32, 12311–12318.
- (36) Kreitman, R. J., Puri, R. K., and Pastan, I. (1994) A circularly permuted recombinant interleukin 4 toxin with increased activity. *Proc. Natl. Acad. Sci. U.S.A.* 91, 6889–6893.
- (37) Hahn, M., Piotukh, K., Borriess, R., and Heinemann, U. (1994) Native-like in vivo folding of a circularly permuted jellyroll protein shown by crystal structure analysis. *Proc. Natl. Acad. Sci. U.S.A.* 91, 10417–10421.
- (38) McWherter, C. A., Feng, Y., Zurfluh, L. L., Klein, B. K., Baganoff, M. P., Polazzi, J. O., Hood, W. F., Paik, K., Abegg, A. L., Grabbe, E. S., Shieh, J. J., Donnelly, A. M., and McKearn, J. P. (1999) Circular permutation of the granulocyte colony-stimulating factor receptor agonist domain of myelopoietin. *Biochemistry* 38, 4564–4571.
- (39) Feng, Y., Minnerly, J. C., Zurfluh, L. L., Joy, W. D., Hood, W. F., Abegg, A. L., Grabbe, E. S., Shieh, J. J., Thurman, T. L., McKearn, J. P., and McWherter, C. A. (1999) Circular permutation of granulocyte colony-stimulating factor. *Biochemistry* 38, 4553–4563.
- (40) Lee, C., Seo, E. J., and Yu, M. H. (2001) Role of the connectivity of secondary structure segments in the folding of α_1 -antitrypsin. *Biochem. Biophys. Res. Commun.* 287, 636–641.
- (41) Nordlund, H. R., Laitinen, O. H., Hytonen, V. P., Uotila, S. T., Porkka, E., and Kulomaa, M. S. (2004) Construction of a dual chain pseudotetrameric chicken avidin by combining two circularly permuted avidins. *J. Biol. Chem.* 279, 36715–36719.
- (42) Mishima, M., Shida, T., Yabuki, K., Kato, K., Sekiguchi, J., and Kojima, C. (2005) Solution structure of the peptidoglycan binding domain of *Bacillus subtilis* cell wall lytic enzyme CwlC: Characterization of the sporulation-related repeats by NMR. *Biochemistry* 44, 10153–10163.
- (43) Huang, C. C., Stricher, F., Martin, L., Decker, J. M., Majeed, S., Barthe, P., Hendrickson, W. A., Robinson, J., Roumestand, C., Sodroski, J., Wyatt, R., Shaw, G. M., Vita, C., and Kwong, P. D. (2005) Scorpion-toxin mimics of CD4 in complex with human immunodeficiency virus gp120 crystal structures, molecular mimicry, and neutralization breadth. *Structure* 13, 755–768.
- (44) Thali, M., Moore, J. P., Furman, C., Charles, M., Ho, D. D., Robinson, J., and Sodroski, J. (1993) Characterization of conserved human immunodeficiency virus type 1 gp120 neutralization epitopes exposed upon gp120-CD4 binding. *J. Virol.* 67, 3978–3988.
- (45) Harbury, P. B., Kim, P. S., and Alber, T. (1994) Crystal structure of an isoleucine-zipper trimer. *Nature* 371, 80–83.
- (46) Dames, S. A., Kammerer, R. A., Wiltschek, R., Engel, J., and Alexandrescu, A. T. (1998) NMR structure of a parallel homotrimeric coiled coil. *Nat. Struct. Biol.* 5, 687–691.
- (47) Selvarajah, S., Puffer, B. A., Lee, F. H., Zhu, P., Li, Y., Wyatt, R., Roux, K. H., Doms, R. W., and Burton, D. R. (2008) Focused dampening of antibody response to the immunodominant variable loops by engineered soluble gp140. *AIDS Res. Hum. Retroviruses* 24, 301–314.
- (48) Dani, V. S., Ramakrishnan, C., and Varadarajan, R. (2003) MODIP revisited: Re-evaluation and refinement of an automated procedure for modeling of disulfide bonds in proteins. *Protein Eng.* 16, 187–193.
- (49) Zhou, T., Xu, L., Dey, B., Hessel, A. J., Van Ryk, D., Xiang, S. H., Yang, X., Zhang, M. Y., Zwick, M. B., Arthos, J., Burton, D. R., Dimitrov, D. S., Sodroski, J., Wyatt, R., Nabel, G. J., and Kwong, P. D. (2007) Structural definition of a conserved neutralization epitope on HIV-1 gp120. *Nature* 445, 732–737.
- (50) Chen, L., Kwon, Y. D., Zhou, T., Wu, X., O'Dell, S., Cavacini, L., Hessel, A. J., Pancera, M., Tang, M., Xu, L., Yang, Z. Y., Zhang, M. Y., Arthos, J., Burton, D. R., Dimitrov, D. S., Nabel, G. J., Posner, M. R., Sodroski, J., Wyatt, R., Mascola, J. R., and Kwong, P. D. (2009) Structural basis of immune evasion at the site of CD4 attachment on HIV-1 gp120. *Science* 326, 1123–1127.
- (51) Walker, L. M., Phogat, S. K., Chan-Hui, P. Y., Wagner, D., Phung, P., Goss, J. L., Wrinn, T., Simek, M. D., Fling, S., Mitcham, J. L., Lehrman, J. K., Priddy, F. H., Olsen, O. A., Frey, S. M., Hammond, P. W., Kaminsky, S., Zamb, T., Moyle, M., Koff, W. C., Pognard, P., and Burton, D. R. (2009) Broad and potent neutralizing antibodies from

an African donor reveal a new HIV-1 vaccine target. *Science* 326, 285–289.

(52) Walker, L. M., Huber, M., Doores, K. J., Falkowska, E., Pejchal, R., Julien, J. P., Wang, S. K., Ramos, A., Chan-Hui, P. Y., Moyle, M., Mitcham, J. L., Hammond, P. W., Olsen, O. A., Phung, P., Fling, S., Wong, C. H., Phogat, S., Wrinn, T., Simek, M. D., Principal Investigators, P. G., Koff, W. C., Wilson, I. A., Burton, D. R., and Poignard, P. (2011) Broad neutralization coverage of HIV by multiple highly potent antibodies. *Nature* 477, 466–470.

(53) Zhou, T., Georgiev, I., Wu, X., Yang, Z. Y., Dai, K., Finzi, A., Kwon, Y. D., Scheid, J. F., Shi, W., Xu, L., Yang, Y., Zhu, J., Nussenzweig, M. C., Sodroski, J., Shapiro, L., Nabel, G. J., Mascola, J. R., and Kwong, P. D. (2010) Structural basis for broad and potent neutralization of HIV-1 by antibody VRC01. *Science* 329, 811–817.

(54) Martin, G., Burke, B., Thai, R., Dey, A. K., Combes, O., Heyd, B., Geonnotti, A. R., Montefiori, D. C., Kan, E., Lian, Y., Sun, Y., Abache, T., Ulmer, J. B., Madaoui, H., Guerois, R., Barnett, S. W., Srivastava, I. K., Kessler, P., and Martin, L. (2011) Stabilization of HIV-1 envelope in the CD4-bound conformation through specific crosslinking of a CD4 mimetic. *J. Biol. Chem.* 286, 21706–21716.

(55) McLellan, J. S., Pancera, M., Carrico, C., Gorman, J., Julien, J. P., Khayat, R., Louder, R., Pejchal, R., Sastry, M., Dai, K., O'Dell, S., Patel, N., Shahzad-ul-Hussan, S., Yang, Y., Zhang, B., Zhou, T., Zhu, J., Boyington, J. C., Chuang, G. Y., Diwanji, D., Georgiev, I., Kwon, Y. D., Lee, D., Louder, M. K., Moquin, S., Schmidt, S. D., Yang, Z. Y., Bonsignori, M., Crump, J. A., Kapiga, S. H., Sam, N. E., Haynes, B. F., Burton, D. R., Koff, W. C., Walker, L. M., Phogat, S., Wyatt, R., Orwenyo, J., Wang, L. X., Arthos, J., Bewley, C. A., Mascola, J. R., Nabel, G. J., Schief, W. R., Ward, A. B., Wilson, I. A., and Kwong, P. D. (2011) Structure of HIV-1 gp120 V1/V2 domain with broadly neutralizing antibody PG9. *Nature* 480, 336–343.

(56) Roehr, B. (2011) Researchers announce first correlates of protection for HIV vaccine. *BMJ [Br. Med. J.]* 343, d5880.

(57) Cohen, J. (2011) AIDS research. Novel antibody response may explain HIV vaccine success. *Science* 333, 1560.